European Journal of Scientific Research
ISSN 1450-216X Vol.22 No.2 (2008), pp.216-231

http://www.eurojournals.com/ejsr.htm

Lattice Boltzmann Method and its Applications to Fluid Flow Problems

Romana Begum
Department of Chemical and Materials Engineering, Pakistan Institute of Engineering and Applied Sciences Nliore, Islamabad, 45650, Pakistan
E-mail: mabdulbasit@gmail.com

M. Abdul Basit
Department of Chemical and Materials Engineering, Pakistan Institute of Engineering and Applied Sciences Nliore, Islamabad, 45650, Pakistan
E-mail: mabdulbasit@gmail.com

Abstract

The main objective of this paper is to demonstrate the validity of lattice Boltzmann me-thod (LBM) for different flows and phase transition process. For the present simulation D2Q9 model has been used. The soundness of LBM has been checked by implementing it on test problems including Plane Poiseuille flow, Planar Couette flow and Lid Driven Cavity flow. The results of these simulations show the capability of present incompressible LBM model in handling both steady and unsteady flows. Blood flow simulation has been performed using Casson's Rheology model and lastly, phase transition process has been simulated using Shan and Chen model. The results obtained for blood flow and phase transition process are in excellent agreement with the analytical results and the results present in literature.

Keywords: Lattice Boltzmann Method, Fluid Flow Problems, Rheology, Poiseuille Flow, Couette Flow

1. Introduction

Lattice Gas Cellular Automata (LGCA) and Lattice Boltzmann Method (LBM) are relatively new and promising methods for the solution of nonlinear partial differential equations and simulation of fluid flows. In the last few years, a remarkable development has been taken place in (LBM) [1-6]. Lattice Boltzmann models have ability to simulate single and multi-phase flows of single and multi-component fluids. Historically the LBM evolves from LGCA which belongs to the class of cellular automata that are used for simulation of the fluid flow phenomena. It represents an idealization of the physical system in which space and time both are discrete. In 1986, Frisch, Hasslacher, and Pomeau and Wolfram proposed the first two-dimensional lattice gas automaton model for the specific purpose of computational fluid dynamics [7]. In 1988, a proposal to use the lattice Boltzmann equation to simulate fluid flow problems was made for the first time. The kinetic nature of LBM has several distinct features different from other computational fluid dynamics (CFD) approaches that are used to solve the Navier Stokes equations. The convection operator in LBM is linear in phase space, similar to that of the Boltzmann kinetic equation, but different than the Euler or the Navier Stokes equations and pressure is obtained through an equation of state, instead of solving a Poisson equation as in the incom-

pressible Navier Stokes equations. LBM uses minimum set of discrete velocities so that the conserved quantities remain preserved throughout the simulation.

Researchers have used LGCA and LBM for a variety of fluid flow problems and geometries. A rich variety of behaviors including unsteady flows, phase separation, evaporation, condensation, cavitations, porous media flows, blood flow simulation, solute and heat transport, buoyancy, multiphase flows, compressible flows and interactions with surfaces can readily be simulated [8-25]. Various fluid flow problems have been simulated using LGCA and results have been compared with experimental investigations [8]. LGCA has been used to investigate flow through geometrically irregular media [11]. An LGCA model with non-ideal equation of state has been presented to simulate the transition from solid to gas phase [12]. LBM has been used to numerically analyze the turbulent shear flows [13]. Results obtained for three-dimensional low Reynolds number flows, using LBM, demonstrate the viability of the method for such flows in complex geometries [14]. LBM is equally applicable for simulation of multiphase flows. LB Models have been formulated for two-dimensional multiphase flows in porous media [15]. Many researchers have formed thermal models to investigate heat conduction process and convective flows by using LBM [20, 23]. LBM has even been used to simulate shock wave phenomena [25].

In present paper two dimensional fluid flow simulations has been performed using D2Q9 LBM model. Poiseuille flow (flow between two parallel plates) is the simplest flow that has been simulated using LBM. In the second step, the velocity boundary condition has been used to numerically solve the two-dimensional Couette flow. Flow in a square cavity that has no analytical solution, has been solved using LBM and the results obtained are in excellent agreement with those in the literature [26]. Casson's Rheology model [27] has been implemented for blood flow simulation by considering it as the non-Newtonian fluid. Lastly, Shan and Chen model [28] has been used to simulate phase transition.

2. Lattice Boltzmann Method

LBM is relatively recent technique that has been shown to be as accurate as traditional CFD methods having the ability to integrate arbitrarily complex geometries at a reduced computational cost. Lattice Boltzmann models vastly simplify Boltzmann's original conceptual view by reducing the number of possible particle spatial positions and microscopic momenta from a continuum to just a handful and similarly discretizing time into discrete steps. Particle positions are confined to the node of a lattice. Variations in momenta that could have been due to a continuum of velocity directions and magnitudes and varying particle mass are reduced to eight directions leading to a D2Q9 model.

3. D2Q9 Model

Fig. 1 shows the cartesian lattice with 8 velocities vectors. Point 0 represents the particles at rest. This model is known as D2Q9 as it is two dimensional and contains nine velocities. The lattice unit *lu* is the fundamental measure of length in LBM, time steps (*ts*) is the time unit and mass unit *(mu)* is used for mass. The velocity magnitude of 1 through 4 velocity vectors is 1 (*lu/ts*) and that of index 5 to 8 is *lu/ts*. These velocities are exceptionally convenient in that all of their x and y-components are either 0 or ±1. Mass of particles is uniformly taken 1 *mu* throughout the domain [29].

Figure 1: D2Q9 lattice and velocities

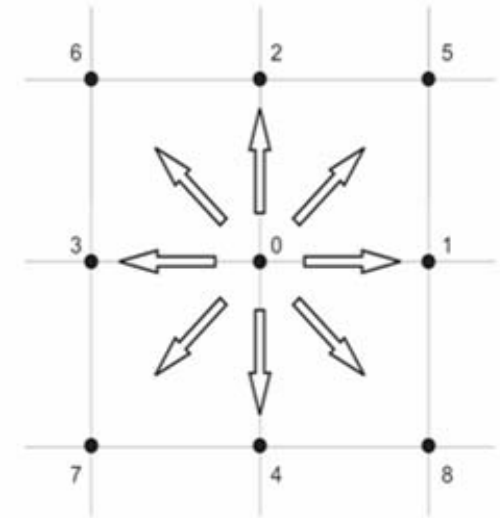

Boltzmann equation, the basic transport equation, is given as:

$$\frac{\partial f}{\partial t} + \vec{v}\nabla f = Q \tag{1}$$

Where f is the distribution function and Q is the collision integral. Here, the external forces have been neglected. The Boltzmann equation with BGK (Bhatnagar Gross Krook) approximation for collision integral reads

$$\frac{\partial f}{\partial t} + \vec{v}\nabla f = -\frac{1}{\tau}(f - f^{eq}) \tag{2}$$

where τ is the collision time and f^{eq} is the equilibrium distribution function.

The distribution function f depends on space, velocity and time i.e. $f(\vec{x},\vec{v},t)$ The v space is discre-tized by introducing a finite set of velocities $\vec{v}_i$ and associated distribution function is governed by the following equation

$$\frac{\partial f_i}{\partial t} + \vec{v}\nabla f_i = -\frac{1}{\tau}(f_i - f_i^{eq}) \tag{3}$$

Macroscopic fluid density is given by

$$\rho = \sum_{i=0}^{8} f_i \tag{4}$$

The macroscopic velocity is the average of the microscopic velocities $\vec{c}_i$ and the directional densities.

$$\vec{u} = \frac{1}{\rho}\sum_{i=0}^{8} f_i \vec{c}_i \tag{5}$$

The basic steps in this method are the streaming and collision processes which are represented in the form of an equation given below:

$$f_i\ (\vec{x} + \vec{c}\Delta t, t + \Delta t) = (1-\omega) f_i\ (\vec{x}, t) + \omega f_i^{eq}(\vec{x}, t) \tag{6}$$

where $\omega = {}^{\Delta t}/_{\tau}$ is relaxation frequency. The left hand side of Eq. (6) is the streaming part and the right hand side is the collision term [30]. Although these can be combined in a single statement as in above equation, collision and streaming steps must be separated if solid boundaries are present because the bounce back boundary condition is a separate collision. Algorithm for this model is shown in Fig. 2.

Collision of the fluid particles is considered as relaxation towards local equilibrium and the equilib-rium distribution for this model are defined as

$$f_i^{eq} = w_i \rho(x)\left[1 + 3\frac{\vec{c}_i \vec{u}}{c^2} + \frac{9}{2}\frac{(\vec{c}_i \vec{u})^2}{c^4} - \frac{3}{2}\frac{\vec{u}^2}{c^2}\right] \tag{7}$$

Figure 2: Algorithm for D2Q9 Model

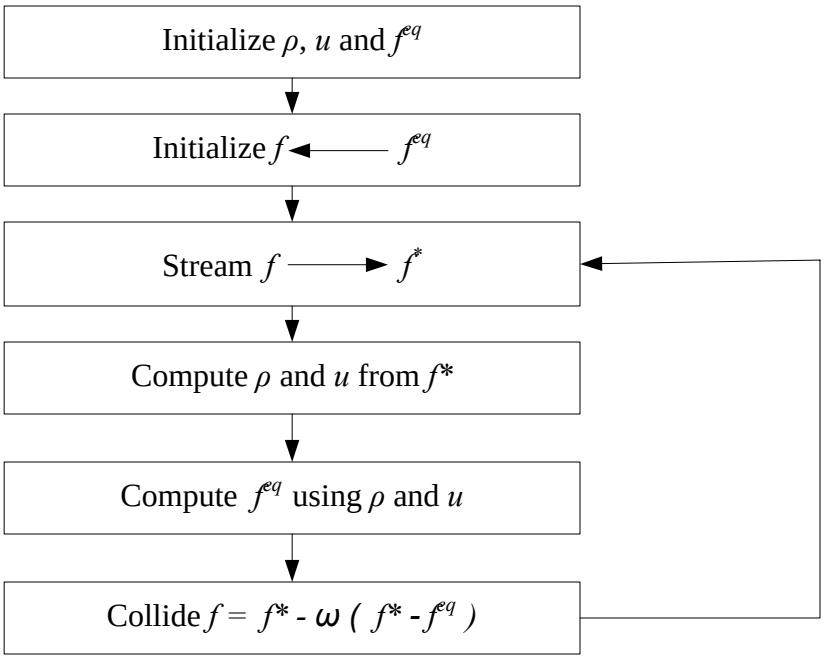

where w_i, the weight, is 4/9 for the rest particles *i*.e. i=0, 1/9 for *i*=1, 2, 3, 4 and 1/36 for *i*=5, 6, 7, 8 and *c* is the lattice speed which is 1 *lu/ts* [30]. Application of multi-scale technique yields the Navier Stokes equation with pressure $p = \rho k_B T/m$ and kinematic shear viscosity is given by

$$\nu = \frac{c^2}{3}\left(\frac{1}{\omega} - \frac{1}{2}\right)\Delta t \qquad 8)$$

4. M Scheme for Blood Flow

Multiphase fluids or so-called 'complex fluids' are common in daily life. The term 'multiphase fluids' which has been used for less than half a century stands for systems with different substances or different phases of matter (solid, liquid or gas) in coexistence. In practice, the underlying multiphase character is often neglected and the system is treated formally as a single phase 'Rheological' or 'non-Newtonian' fluid. In many applications with low volume fraction of particles, droplets or bubbles, the system may indeed behave like a single-phase fluid.

Blood is a suspension of formed blood cells and some liquid particles in an aqueous solution (the plasma). The most important mechanical property of blood that influences its motion is the apparent viscosity η, which relates the shear rate $\dot{\gamma}$ and the shear stress σ. If this relationship satisfies the Newton's law of viscosity then the fluid is known as a Newtonian fluid and if not then it is known as non-Newtonian fluid. There are different models which are used to describe the behavior of blood flow and one of them is the Casson's Rheology model.

5. Casson's Rheology Model

The Casson's model is valid under specific conditions and should not be regarded as an exhaustive description of blood. Blood with small shear rates $\dot{\gamma} \leq 10s^{-1}$ and hematocrit less than 40% can be described by Casson's equation

$$\sqrt{\eta|\dot{\gamma}|} = \begin{cases} \sqrt{\sigma} - \sqrt{\sigma_y} & \text{if } \sigma \geq \sigma_y \\ 0 & \text{otherwise} \end{cases} \qquad (9)$$

where η is a constant viscosity, σ the shear stress, $|\dot{\gamma}|$ is the shear strain rate defined as $2|S_{\alpha\beta}|$ and σ_y is the so called yield stress. This relation exp`resses the fact that below some yield stress, no strain rate is observed. The quantity σ_y is of the order of 0.05 dyn/cm^2 and is almost independent of the temperature in the range 10-37$^{\circ}C$. Without fibrinogen, a suspension of red cells has zero yield stress [27].

From Casson's model it is concluded that at higher shear rate, blood behaves like a Newtonian fluid. The final form of the Casson's model is

$$\mu = \begin{cases} \dfrac{(\sqrt{\sigma_y} + \sqrt{\eta|\dot{\gamma}|})^2}{|\dot{\gamma}|} & if\ \sigma > \sigma_y \\ \infty & if\ \sigma \leq \sigma_y \end{cases} \tag{10}$$

where μ is a variable viscosity, which is a function of yield stress σ_y, constant viscosity η and $|\dot{\gamma}|$ shear strain rate.

5.1. Lattice Boltzmann Casson's Model

Numerical simulations offer a promising way to investigate blood flow in complex situations. The LBM has proved to be a flexible and powerful blood flow solver. In LB scheme the stress tensor is given by

$$\prod \alpha\beta = \sum_i v_{i\alpha} v_{i\beta}(f_i - f_i^{(0)}) \tag{11}$$

Strain rate tensor is related to stress tensor by

$$|S_{\alpha\beta}| = \frac{-3\prod \alpha\beta}{2\rho\Delta t\tau_\mu v^2}$$

$$|\dot{\gamma}| = 2\sqrt{S_{\alpha\beta}S_{\alpha\beta}}$$

$$\sigma = \sqrt{\prod \alpha\beta \prod \alpha\beta} \tag{12}$$

The final form for viscosity is

$$\sqrt{\frac{\mu}{\eta}} = \frac{1}{\theta}\left[1 + \sqrt{\theta\left[1 + \frac{\rho\Delta t v^2}{6\eta}(1-\theta)\right]}\right] \tag{13}$$

where $\theta = \sigma_y/\sigma$ Eq (13) is valid when $\theta \ll 1$. Otherwise from Casson's Rheology model the viscosity is infinite. In the numerical model a ceiling viscosity has been introduced for small shear stress values. This cut off viscosity is reached when $\sigma = \sigma_y + \varepsilon$ where ε is a small positive real number [27].

6. Shan and Chen Model

The true strength of LBM lies in its ability to simulate multiphase fluids. There are different LB models used to simulate the multiphase flows. A complete description of multiphase models can be found in [31-37]. No general consensus has emerged as yet on which one of these methods should be recommended as the best LBE (Lattice Boltzmann Equation) solution method for multiphase problems.

Phase transition is a process in which a liquid changes into its vapor state or from vapor state to liquid state. The basic parameter which is responsible for this conversion is the temperature. In single component multiphase (SCMP) model proposed by Shan and Chen, interaction parameter G plays the same role as that of temperature in non-isothermal models. The results presented here depict the ability of Shan and Chen model to simulate the phase separation process.

Shan and Chen [28] suggested the use of microscopic interaction potential among particles in LBM. To simulate non ideal gases and their mixtures, long range interactions among the particles must be in-cluded. For our purpose, a cohesive force added to nearest neighbor fluid particles and for the D2Q9 model this force is given by

$$F(\vec{x}, t) = -G\psi(\vec{x}, t)\sum_{i=1}^{8} w_i \psi(\vec{x} + \vec{c}\Delta t, t)\vec{c}_i \quad (14)$$

where G is the interaction strength, w_i is 1/9 for i=1, 2, 3, 4 and 1/36 for i=5, 6, 7, 8 and ψ is the interaction potential and is given as:

$$\psi(\rho) = \psi_0 e^{(-\rho_0/\rho)} \quad (15)$$

where ψ_0 and ρ_0 are arbitrary constants. Different forms of interaction potential are in use. According to Shan and Chen the only restriction for potential is that, this potential must be monotonically increasing and bounded [29]. Other commonly used form for the interaction potential is [30]

$$\psi(\rho) = \rho_0\left[1 - e^{(-\rho_0/\rho)}\right] \quad (16)$$

When attractive force exists between particles, G is taken less than zero. The force is stronger when density is higher, so the dense region (liquid) experiences a stronger cohesive force than vapor, which leads to surface tension phenomenon. The attractive force incorporated in the model is used to find equilibrium velocity u^{eq} which is needed to calculate the equilibrium distribution function Eq. (7).

$$u^{eq} = u + \Delta u = u + \frac{\tau F}{\rho} \quad (17)$$

The attractive feature of this model is that phase separation takes place spontaneously whenever the interaction strength G exceeds a critical value thus fitting naturally the physical notion of G as an inverse effective temperature of the system. Here only attractive force has been considered and the repulsive force that dominates the Vander Waals gas model when a gas is compressed has been neglected in this single component multiphase model.

7. Results and Discussion

The simplest LBM models that can be implemented based on the concepts presented in the preceding discussion are the single component single phase models and the single component multi phase models. These models are implemented for different fluid flow problems, both for Newtonian and non Newtonian fluids. The results are discussed below.

7.1. Plane Poiseuille Flow

The Poiseuille flow is the simplest flow simulated by LBM. The problem is solved analytically by considering maximum velocity U_0 with constant pressure gradient. The flow is one dimensional incompressible and laminar. No slip boundary conditions are applied at the walls. The analytical solution gives a parabolic velocity profile. The velocity has maximum value in the centre and becomes zero at the walls of the channel.

7.1.1. Mesh and Solution Parameters

The mesh used for this simulation has twenty nodes in y-direction and thirty nodes in x-direction. The mesh is taken uniform both in x and y-directions. Maximum velocity of flow is 0.1 *lu/ts*. The simulation performed by using LBM assumes the full way bounce back boundary conditions at upper and lower plate. Periodic boundaries have been used in the flow direction hence the flow that leaves the domain, reenters on the opposite end of the channel. Hence the system is infinite in the flow direction, so there are no entry or exit effects. It is critical that lattice velocities be restricted to remain less than or equal to 1 *lu/ts*. This is a consequence of the low Mach number approximation that allows LBM to simulate hydrodynamics. The relaxation parameter *(ω)* was taken as 1.8. Density used during simulation was 0.1. The number of time-steps used was 10000. Forcing function which starts the flow between plates was 3.81e-06.

7.1.2. Discussion

The Fig. 3 shows the comparison of LBM and analytical results, which are in good agreement. Only difference comes at the walls due to the use of full way bounce back boundary conditions (Fig. 3). The relaxation parameter in LBM is a basically convergence parameter, so to check its effect different velocity profiles have been plotted for different values of relaxation parameters (Fig. 4). As the value of ω lies in the range $1<\omega<2$ so when relaxation parameter approaches close to 2, the instability in flow occurs.

The instabilities in the flow can be triggered at much low Reynolds number (*Re*) in the presence of obstacles. An obstacle of 4 *lu* was introduced at $x = 5$ vertically (Fig. 5). When *Re* increases from creeping flow regime, separation occurs and eddies are formed behind the obstacle [29, 30]. These elongate as *Re* increases up to 50. This flow is obviously much richer than the laminar Poiseuille flow since all non linear terms now are in action.

7.2. Planar Couette flow

Planar Couette flow is the flow between two parallel plates such that one is moving and other is at rest. The Couette flow is simulated both for steady and unsteady case for constant pressure gradient by using LBM.

7.2.1. Mesh and Solution Parameters

The mesh used for discretization of continuous fluid has been kept uniform in both directions. The number of nodes taken in horizontal direction are 30 and in vertical direction are 20. The velocity of upper plate has been kept as 0.15 *lu/ts* in positive horizontal direction with no pressure gradient. The lower plate is at rest. At inlet and outlet periodic boundary conditions are used. At upper and lower plate full way bounce back boundary conditions have been applied. The relaxation parameter *(ω)* was 1.85. Density used during simulation was 0.1. Simulation was run for 20000 time steps.

Figure 3: Velocity profile by analytical and LBM

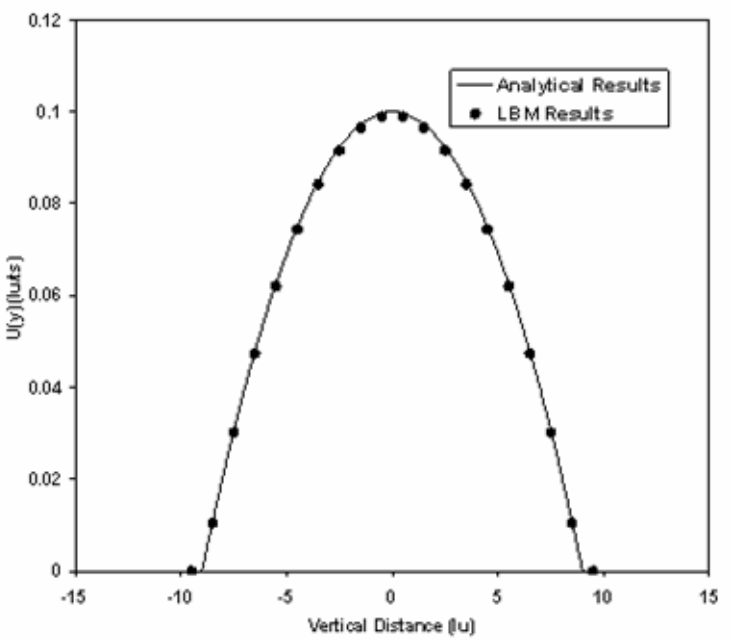

Figure 4: Velocity profile for different values of ω

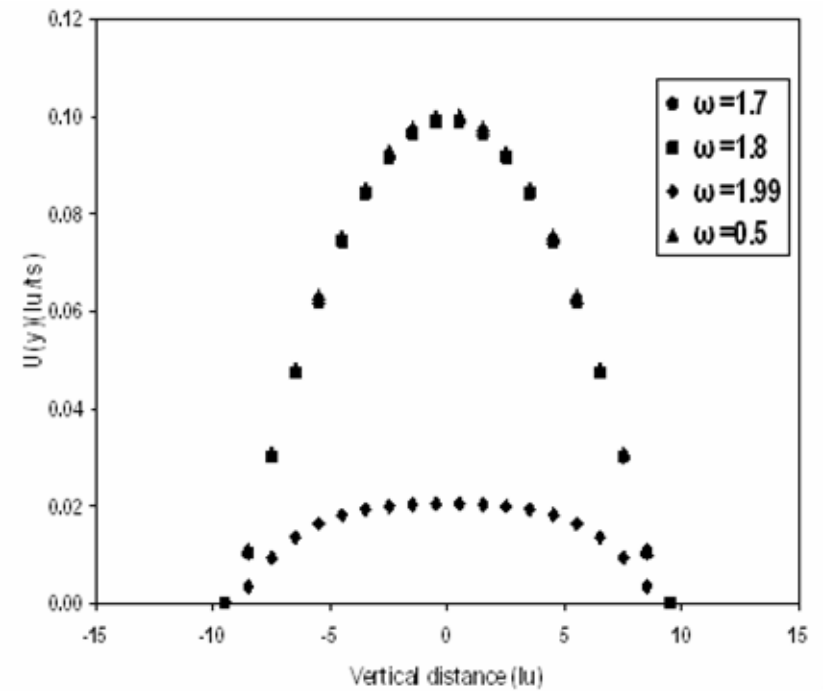

Figure 5: Eddies at Re = 127 for obstacle at x= 5

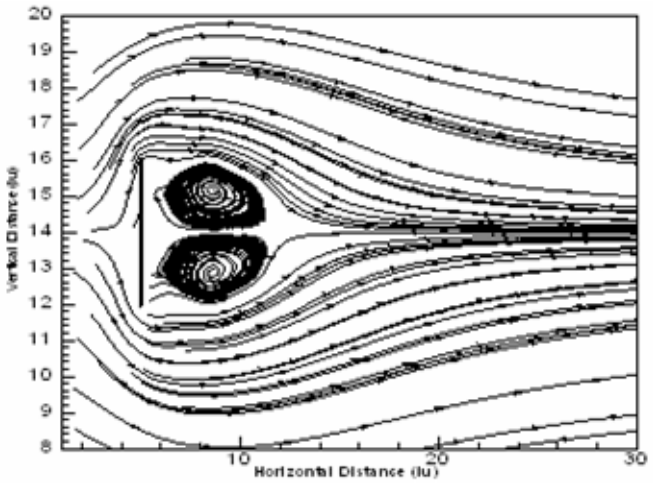

7.2.2. Discussion

The velocity profiles have been plotted in Fig. 6. The line depicts analytical solution and discrete points are LBM results for steady state. Separation between the plates has been plotted along x-axis and velocity along vertical axis. It is quite easy to get transient solution for this flow problem using LBM as it is inherently a transient scheme. A detailed comparison of unsteady state velocity profiles for both analytical and LBM results have been shown in Fig. 7. As the number of time steps increases the velocity profile approaches the steady state velocity profile.

7.3. Lid Driven Cavity flow

The lid driven cavity flow is always an important flow to check the validity of any numerical scheme because it has no analytical solution. An incompressible fluid is bounded by a square enclosure and the flow is driven by a uniform translation of top lid.

7.3.1. Mesh and Solution Parameters

For the square cavity, mesh size of 256 nodes has been taken both in horizontal and vertical directions. The present simulation uses Cartesian coordinate system with origin located at lower left corner. The Reynolds number is determined by using the $Re = UL/v$, where U is the velocity of upper lid, L is the number of lattice sites on one side of cavity and v is the kinematic viscosity of fluid present in the cavity. Density is taken to be 0.1 throughout the simulation. The relaxation parameter (ω) was taken as 1.8

Figure 6: Comparison of horizontal velocity profile

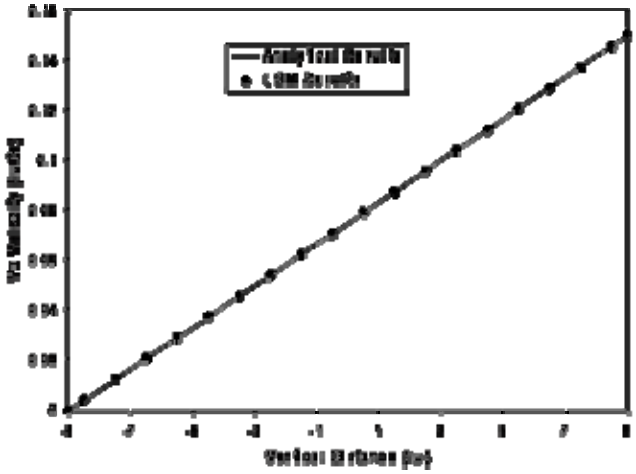

Figure 7: Transient Horizontal Velocity profiles for Couette Flow

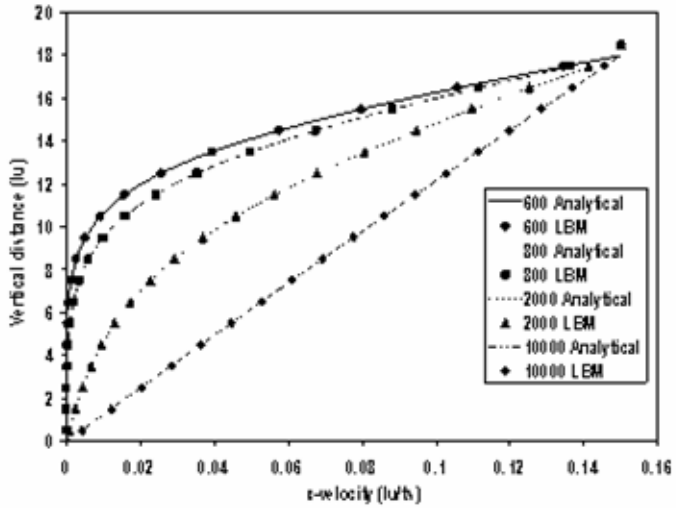

At the three walls, other than the top wall full way bounce back boundary condition has been used. The top wall moves from left to right. The results have been obtained for different values of Reynolds numbers .i.e. Re = 100, 800 and 4000 on a 256×256 lattice [38]. In all cases steady state solutions were obtained, and as the Re was increased towards 4000 the steady state was achieved in larger number of time steps. The two upper corners are singular points which are considered as part of

moving lid in the simulations. Initially the velocity at all the nodes, except the top nodes, is set to zero. Then the equilib-rium particle distribution function is calculated and is set equal to non equilibrium distribution func-tion. The evolution of distribution function can then be found by a succession of streaming and relaxa-tion processes. At the end of each streaming and collision process cycle, f_i at the top is set to equilib-rium state.

7.3.2. Discussion

Fig. 8a-c shows the stream traces in the cavity for the *Re* considered. Flow structure is in good agreement with the previous work of Benjamin and Denny [26]. In addition to the primary, centre vortex, a pair of counter rotating eddies of much smaller strength develop in the lower corners. For low *Re*, the centre of primary vortex is located at the mid width. As *Re* increases the primary vortex-centre moves towards the right and becomes increasingly circular.

The drag coefficient on the top wall has been calculated for the *Re* of present simulations by using the following relation.

$$C_d = \frac{F_d}{\bar{\rho} U^2 L} \tag{18}$$

where $\bar{\rho}$ is the average density and U is the velocity of top wall and L is the number of lattice sites in any direction and $F_d = \int_0^L \tau_{yx}\, dx$ is the drag force. τ_{yx} is the stress on the top wall. Fig. 9 shows the plot of drag coefficient for different values of *Re*.

Figure 10a-c displays the pressure contours. The contours are obtained for different values of *Re.* From the closed pressure contours, it can be concluded that inviscid core region grows with the increasing *Re*. In LBM the pressure is obtained by $p = \rho c_s^2$ where c_s, is the speed of sound. Due to the excellent agreement of all the results of present work with the literature proves that LBM is a persuasive tool to simulate the incompressible flows. The pressure contours obtained are in agreement with those presented in [31].

Velocity components along horizontal and vertical centre lines for several values of *Re* are shown in Figs. 11 and 12. The velocity profiles change from curved at lower values of *Re* to linear for higher *Re* values.

Figure 8: Stream traces (a) Re =100, (b) Re=800, (c) Re=4000

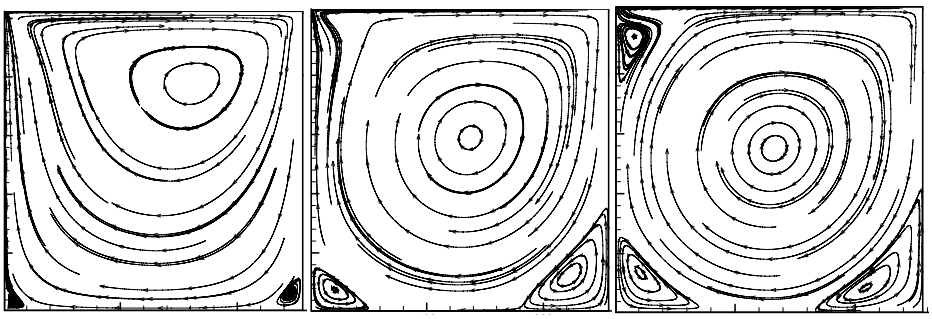

a b c

Figure 9: Drag Coefficient for different values of *Re*.

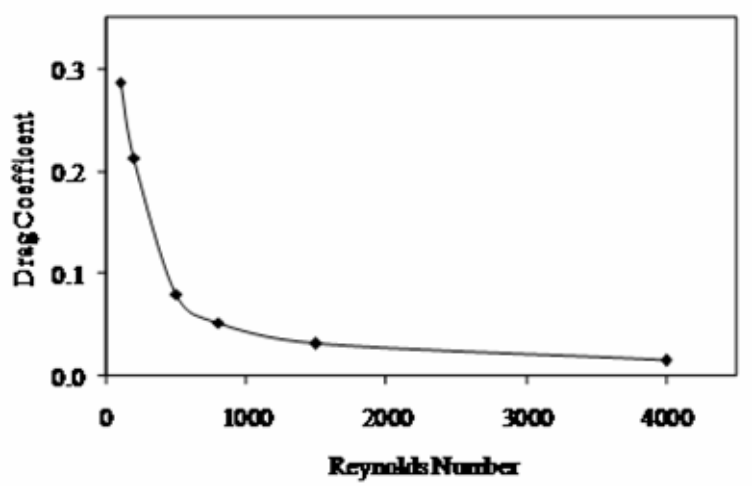

Figure 10: Pressure Contours (a) *Re* =100, (b) *Re*=800, (c) *Re*=4000

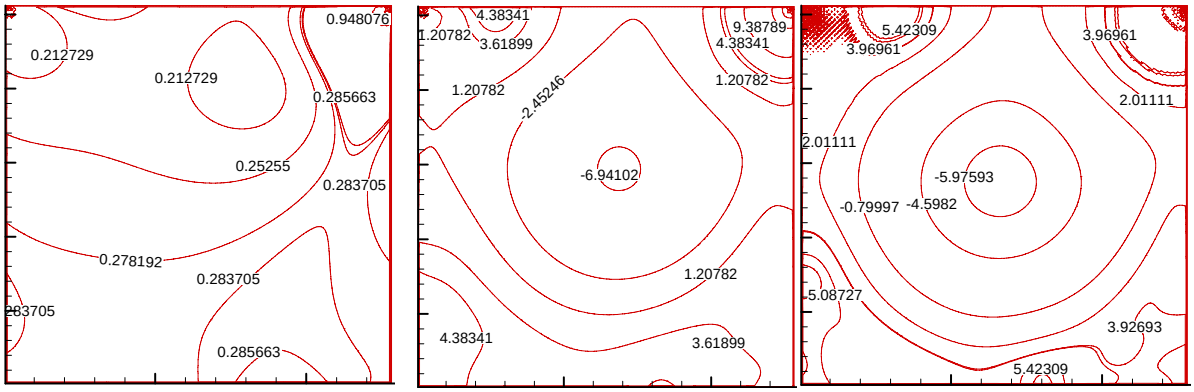

Figure 11: Horizontal velocity through the geometric centre of cavity

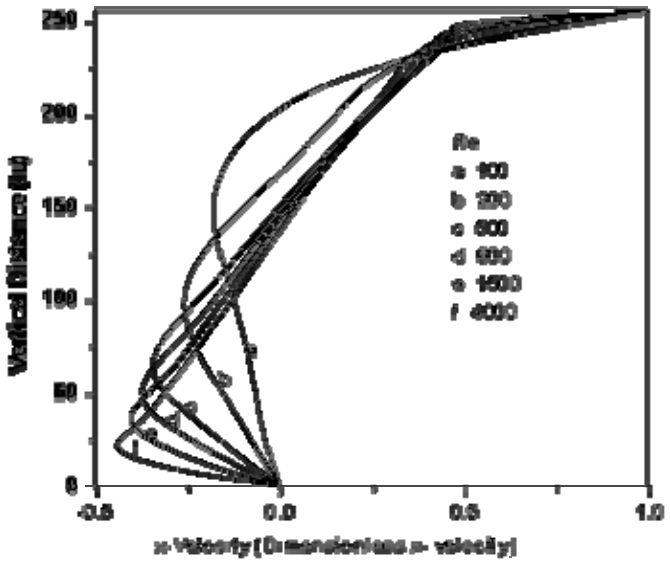

Figure 12: *y*-velocity through the horizontal geometric centre of cavity

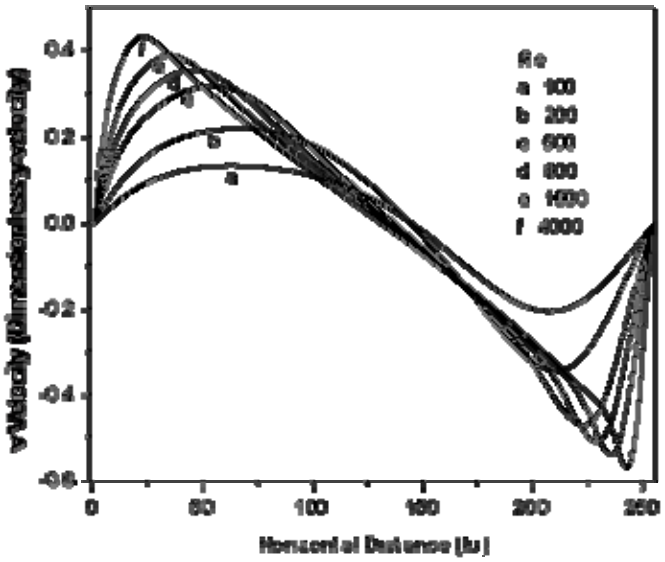

7.4. Blood Flow

The blood flow simulation has been performed by using LB Casson's model. In present work blood has been considered as a non-Newtonian fluid. In the case of non-Newtonian Rheology the viscosity depends on strain rate i.e. the relaxation parameter is a function of shear stress. So during a particular simulation the relaxation parameter varies and does not remain constant as in the case of Newtonian fluid.

7.4.1. Mesh and Solution Parameters

The mesh for this problem has 30 nodes in x-direction and 40 nodes in y-direction. The fluid has been placed between two parallel plates, separated by a distance of 39 lattice units. The upper and lower plates are stationary. The flow is started in the discretized domain by introducing a constant force. At the inlet and outlet, periodic boundary conditions have been applied. At upper and lower plate full way bounce back boundary conditions have been used.

Figure 13: Comparison of x-velocity profile of blood and Newtonian fluid

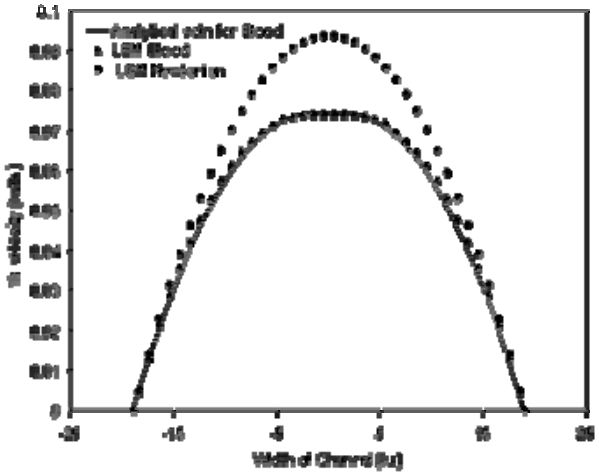

Figure 14: Variation of relaxation time across the channel width

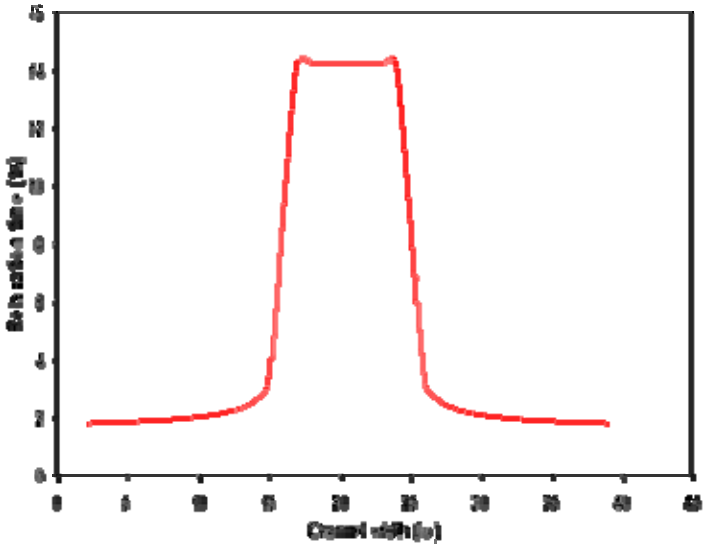

Forcing used to start the flow is taken as 0.00000381. The density was taken as 0.1 and it remained constant during the simulation. The relaxation parameter was set equal to 1 initially. Yield stress used in Casson's model was taken to be 0.0001.

7.4.2. Discussions

Figure. 13 shows the comparison of horizontal velocity profile for blood and Newtonian fluid depicting that the maximum velocity obtained in the case of blood flow is smaller than that of the Newtonian fluid. This is due to more viscous nature of blood.

Figure. 14 shows the variations of relaxation parameter across the channel width. The relaxation parameter is constant in the middle of channel and near the upper and lower plate it has almost expo-nential behavior.

7.5. Phase Transition

Multiphase flows play an important role in daily life, and its simulation is a challenging task. Multiphase flows are characterized by phase transition process. In the present paper the simulation of phase transition is performed using Shan and Chen model [28].

7.5.1. Mesh and Solution Parameters

To perform the simulation, a uniform mesh of 150×150 lu2 has been used. The whole domain was initialized with an average density of 200 mu/lu2and was perturbed with a random number in the interval [0, 1] at each node. = 4 and = 200 are taken during the simulation. For phase transition simula-tion value of G was chosen equal to -120. For simplicity a periodic domain was assumed. Relaxation time was taken as 1 for all the simulations.

7.5.2. Discussion

Results for phase transition of a liquid drop immersed in its own vapors are being discussed here:

Phase Transition

Evolution of mass density distribution, which leads to the phase transition, has been performed for var-ious time steps and has been shown in Fig.15 (a-i). Dark color specifies a region with higher density and hence is identified as liquid while white region depicts the vapor phase with a lower density. It can be observed that at the start, the phase transition is very quick but becomes slower due to the fact that large amount of small droplets start competing for those liquid particles which are in

vapor phase. In the present case, phase transition leads to a single drop of liquid in a vapor atmosphere. Whether liquid drops or vapor bubbles are formed, as a result of phase transition process, depends on the initial density selected. In Fig.4 it can be seen that the smaller droplets are more unstable than the large droplets. This is due to the surface tension effects on the interface with a larger curvature.

Figure 15: Phase transition for $\psi_c = 4$ and ρ_v =200 for different time steps (a) 1, (b) 100, (c) 500, (d) 1000, (e) 2000, (f) 4000, (g) 8000, (h) 15000, (i) 30000

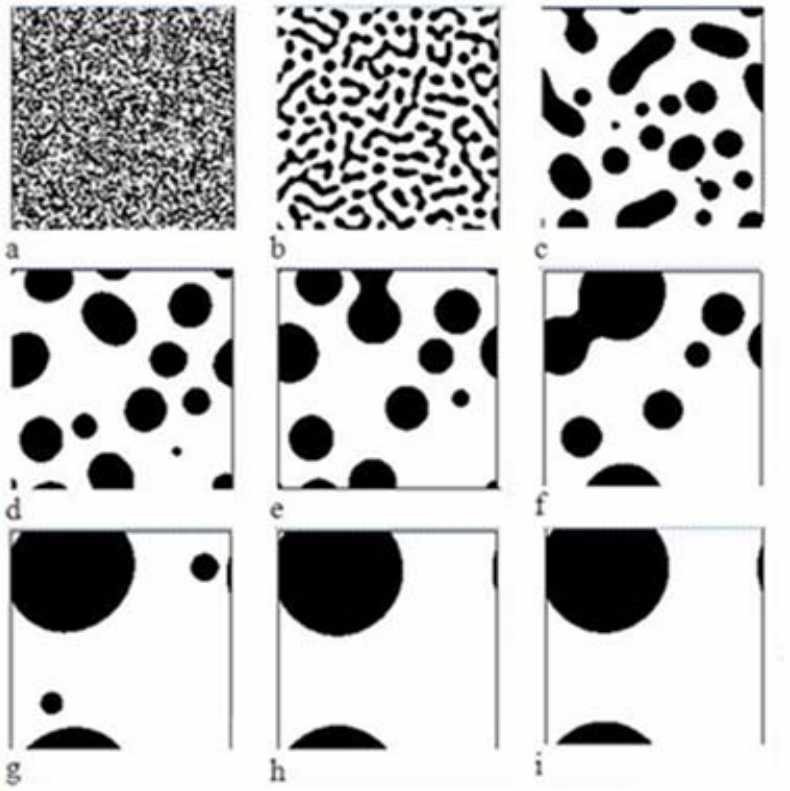

8. Conclusions

In the present paper the Lattice Boltzmann method has been used to simulate different fluid flow problems and phase transition process. The results obtained in all cases are in good agreement with the analytical results showing the validity of LBM for incompressible flows. The results of Lid Driven Cavity flow are also in excellent agreement with the results present in the literature [26]. The LBM Casson's model has been implemented for the simulation of blood flow by considering it as a non-Newtonian fluid. It can be concluded that relaxation parameter is the basic convergence parameter in this method which remains constant throughout the domain for the simulation of Newtonian fluid but it changes at each time step in the case of non Newtonian fluid. Shan and Chen model has been used to simulate the multiphase phenomenon and the results are in excellent agreement with the results present in literature [28]. LBM can be considered to be an efficient numerical method for simulation of fluid flow problems.

References

[1] G. McNamara and G. Zanetti, Phys. Rev. Lett. **61**, 2332,1988

[2] J. Higuera, S. Succi, and R. Benzi, Europhys. Lett. **9**, 345,1989

[3] H. Chen, S. Chen, and W. H. Matthaeus, Phys. Rev. A **45**, R5339 ,1991

[4] Y. H. Qian, D. d'Humie`res, and P. Lallemand, Europhys. Lett. 17, 479 ,1992

[5] Lattice Gas Methods for Partial Differential Equations, edited by Gary D. Doolen, Addison-Wesley, Redwood City, CA, 1990

[6] Lattice Gas Methods: Theory, Applications, and Hardware, edited by Gary D. Doolen, MIT, Cam-bridge, 1991

[7] Dieter A. Wolf Gladrow, Lattice Gas Cellular Automata and Lattice Boltzmann Models, Lectures Notes in Mathematics, 1st Edition, Springer Verlag Berlin Heidelberg, New York, 2000.

[8] Special issue on lattice-based models and related topics, edited by J. L. Lebowitz, S. A. J. Stat. Phys. 81, 1995

[9] M. Sahimi, Flow phenomena in rocks: from continuum models to fractals, percolation, cellular au-tomata and simulated annealing, Rev. Mod. Phys. 65(4), 1393, 1993.

[10] J. Bear, Dynamics of Fluids in Porous Media, Elsevier, New York, 1972

[11] S. Succi, E. Foti and M. Gramignani, Flow through geometrically irregular media with lattice Gas Automata, Meccanica 25, 253, 1990.

[12] S. Chen, K. Diemer, G. Doolean, K. Eggert, C.Fu, S. Gutman and B. Travis, Lattice gas models for non ideal fluids, Physica D 47, 97, 1991.

[13] R. Benzi, S. Succi, and M. Vergassola, Phys. Rep. 222, 145, 1992.

[14] E. Foti, S Succi and F. Higuera, Three dimensional flows in complex geometries with the lattice Boltzmann method, Europhys. Lett. 10(5), 433, 1989.

[15] A. Gunstensen, D. Rothman, S. Zaleski and G. Zanetti, Lattice Boltzmann model of immiscible fluids, Phy. Rev. A 43(8),4320, 1991.

[16] D. Rothman and S. Zaleski, lattice gas models of phase seperation, Rev. Mod. Phys.66, 1417, 1994.

[17] A. Gunstensen, and D. Rothman, Lattice Boltzmann studies of immiscible two phase flows through porous media, Phys. Rev. A 43, 4320, 1991

[18] H. Shan and H. Chen, Simulation of non ideal gas and liquid gas phase transitions by the Lattice Boltzmann equations, Phys. Rev. E 49, 2941, 1995.

[19] M. Swift, W. Osborne and J. Yeomans, Lattice Boltzmann simulations of non ideal fluids, Phys. Rev.Lett.75, 830, 1995.

[20] X. Shan, Simualtion of Rayleigh Benard convection using Lattice Boltzmann method, Phys. Rev. E 55, 2780, 1997.

[21] K. Xu and L. S. Luo, Connection between lattice Boltzmann equation and beam scheme. Int. J. Mod. Phys. C 9(8), 1177, 1998.

[22] F. Alexander, S. Chen and J. Sterling, Lattice Boltzmann thermo hydrodynamics, Phys. Rev. E 53, 2298, 1993.

[23] Y. Chen, H. Ohashi and M. Akiyama, Thermal lattice Bhatnagar Gross Krook model without non linear deviations in macrodynamic equations, Phys. Rev. E 50, 2776, 1994.

[24] Y. Chen, Lattice Bhatnagar Gross Krook Methods for Fluid Dynamics: Compressible, Thermal and Multiphase Models, Ph.D. Thesis Dept. of Quantum Engineering and System Science, University of Tokyo, 1994.

[25] G. Yan, Y. Chen and S. Hu, Simple lattice Boltzmann for simulating flows with shock waves, Phys. Rev. E 59, 454, 1999.

[26] S. H. Qisu Zou et al, "Simulation of Cavity Flow by the Lattice Boltzmann Method", Journal of Computational Physics, Volume 118 Page 329-347, Nov. 1994

[27] Rafik Ouared and Bastien Chopard, “Lattice Boltzmann Simulations of Blood Flow Non Newto-nian Rheology and Clotting Processes,” Journal of Statistical Physics, Vol.121, Nos.112, October 2005.
[28] Shan X and Chen H, “Lattice Boltzmann model for simulating flows with multiple phases and components”, Physical Review, Vol.47, No.3 p.1815-1817, 1993
[29] Michael C.Sukop, Daniel T.Thorne, Jr., Lattice Boltzmann Modeling An Introduction for Geo-scientists and Engineers, 1st Edition, Springer Verlag Berlin Heidelberg, 2006
[30] Sauro Succi, The Lattice Boltzmann Equation for Fluid Dynamics and Beyond, 1st Edition, Clar-endon Press Oxford, 2001
[31] J. L. Sohn, Int. J. Numer. Methods Fluids , Volume 8, Page1469,1988
[32] Rothman D.H., “Cellular Automata Fluids: A Model for Flow in Porous Media”, Geophysics 53: 509-518, 1988
[33] Appert C. and Zaleski S., “Lattice Gas with Liquid Gas Transition”, Phys Rev Lett, 64:1-4, 1990.
[34] Swift M.R., Orlandini E, Osborn W. R. and Yeomans J.M., “LB Simulations of Liquid Gas and Binary Fluid”, Phys Rev E 54:5041-5052, 1996.
[35] He X, and Doolen G. D., “Thermodynamic foundations of kinetic Theory and LB Models for Multiphase Flows”, J Stat Phys 107:309-328, 2002.
[36] Zhang R, and Chen H, “LBM for Liquid Vapor Thermal Flows”, Phys Rev E 67, 2003
[37] D. Rothman and S. Zaleski,”Lattice gas models of phase separation”, Rev. Mod. Phys. 66, 1417, 1999
[38] Begum, R., Basit, M. A., Chughtai, I.R.,” Lattice Boltzmann Simulation of Flow in a Lid Driven Square Cavity”, Science International Lahore Pakistan.